View metadata, citation and similar papers at core.ac.uk

brought to you by CORE

provided by NASA Technical Reports Server

N87-26428

PHOTOVOLTAIC CONVERSION OF LASER POWER TO ELECTRICAL POWER

Gilbert H. Walker
NASA Langley Research Center
Hampton, Virginia

and

John H. Heinbockel
Old Dominion University
Norfolk, Virginia

Photovoltaic laser to electric converters are attractive for use with a space-based laser power station. This paper presents the results of modeling studies for a silicon vertical junction converter used with a Nd laser. A computer code was developed for the model and this code was used to conduct a parametric study for a Si vertical junction converter consisting of one p-n junction irradiated with a Nd laser. These calculations predict an efficiency over 50 percent for an optimized converter.

INTRODUCTION

Space-based laser power stations will require converters at the receiving spacecraft to convert the laser radiation to electricity. Photovoltaic converters are promising devices for this use (ref. 1). Special considerations must be given to the laser wavelength and to the laser power density. Figure 1 shows some laser photon energies compared to selected semiconductor bandgap energies. The semiconductor, for use as the photovoltaic converter, must be chosen so that its bandgap energy is slightly less than the energy of the laser photons to be converted into electricity (ref. 2). Incident power densities may be as high as 1×10^3 watts cm^{-2}. In a previous paper (ref. 2) vertical junction converters were suggested as appropriate for use as laser photovoltaic converters. A promising solar-pumped laser for use on a laser power station is a Nd laser (ref. 3). From figure 1, silicon is the appropriate semiconductor for use with a Nd laser. The Si bandgap energy is 1.11 eV, slightly less than the 1.17 eV energy of the photons from the Nd laser. The maximum power density assumed in this study is 1×10^3 watts cm^{-2} at 1.06 μm or 3.47×10^{21} photons cm^{-2} sec^{-1}. The photons are absorbed at an appreciable depth into the semiconductor rather than absorbed near the top surface. This paper describes a model developed to study vertical junction laser-photovoltaic converters and the application of this model to the Nd laser-Si single vertical junction photovoltaic converter.

MODEL

The model (described in detail in Appendix A) for this vertical junction converter uses the device geometry shown in figure 2 and assumes a generation rate at a depth β given by

$$g(\beta) = \phi_0(1 - R_e)\ \alpha\ e^{-\alpha\beta} \quad (1)$$

where ϕ_0 is the number of incident photons [cm^{-2} sec^{-1}], α is the absorption coefficient [cm^{-1}], and R_e is the reflection coefficient. The basic equations for a n/p device involve the photocurrent from the n and p materials as well as the photocurrent from the depletion regions. Current is assumed to flow in sheets parallel to the top surface of the converter; thus, the model contains no diffusion between sheets. These currents, when summed, produce the total short circuit current. At this depth (β), we assume that a narrow strip exists which behaves like a conventional photoconverter. The short circuit current and dark currents are used in the equivalent circuit diagram of figure 3 together with the effects of the series resistance (R_s) and shunt resistance (R_{sh}) to obtain a current-voltage relationship.

The temperature of the photoconverter is determined by the balance between the rate of heat production due to the fraction of absorbed laser power which is degraded to heat and the rate of heat loss by conduction. The model includes a heat-transfer calculation from the converter to a heat pipe at the back face of the device. The device temperature may be controlled by varying the heat pipe temperature and the heat-transfer coefficient.

APPROACH

Using the computer code developed for the model, a study of the Nd laser-Si vertical junction photovoltaic converter was conducted. (Table I shows the baseline parameters used in this study.) In this study, these baseline parameters were varied individually in order to determine the optimum value for each parameter.

RESULTS

Wavelength

Figure 4 shows the efficiency as a function of wavelength. The efficiency varies from 8 percent at a wavelength of 0.6 μm to 54 percent at a wavelength of 1.05 μm. At the wavelength of the Nd laser (1.06 μm), the converter efficiency is 53 percent at baseline conditions.

Converter Width

Figure 5 shows the effect of increasing the converter width with the p-n junction located 10 μm from one edge. The efficiency is highest for the smaller widths. The efficiency is about 56 percent for a width of 20 μm, and it remains above 50 percent for widths as great as 55 μm. Based on these data, for a small sacrifice of efficiency, wider single-crystal converters can be used. Thus, for a series-connected, multijunction device, a range of currents and voltages can be achieved. Although smaller width converters can produce slightly higher efficiencies, for the purpose of this study, the optimum achievable width is 20 μm.

Junction Position

The efficiency for the baseline converter is a strong function of the width of the p-region (here called junction position). Figure 6 shows this efficiency as a function of junction position for the 20 μm wide baseline converter. As the junction position is changed from 2 μm to 16 μm, the efficiency increases from approximately 38 percent to 57 percent. As the junction position is moved to greater values, the width of the p-region increases. The p-region has longer minority carrier diffusion lengths thus accounting for an increased efficiency (ref. 4). For our optimum cell, the junction position is chosen to be 16 μm.

Converter Thickness

Figure 7 shows the efficiency as a function of converter thickness for the baseline converter. Thickness is the distance in the direction of travel of the laser light within the converter. The efficiency increases from less than 2 percent at a thickness of 1×10^{-3} cm to greater than 53 percent at a thickness of 1.5×10^{-1} cm. The photons from the 1.06 μm laser are absorbed relatively deep in the semiconductor. From this the thickness of our optimum cell is 1.5×10^{-1} cm.

Temperature and Heat-Transfer Coefficient

The interface between the heat pipe and the converter must be an electrically insulating, thermally conducting surface. However, the major emphasis of our investigations has been on the structure and performance of the converter. The baseline heat-transfer coefficient was chosen to be 100 cal sec^{-1} cm^{-2} $°C^{-1}$, corresponding to a layer of insulating material. By varying the heat-transfer coefficient and the heat-pipe temperature, the converter temperature can be varied. Figure 8 shows the efficiency as a function of temperature. The efficiency at our baseline temperature of 293 K is 52 percent. This efficiency decreases to 28 percent at 500 K with a temperature coefficient of approximately -0.13 percent/K. Our optimum cell uses a heat-transfer coefficient of 40 cal sec^{-1} cm^{-2} $°C^{-1}$ to maintain the operating temperature of 293 K.

Power Density

Lasers in space for power-transmission applications may provide power densities up to 1×10^3 watt/cm^2 at the receiver. Figure 9 shows the efficiency as a function of power density for baseline conditions. The efficiency increases from about 41 percent at 1 watt/cm^2 to about 53 percent at 1×10^3 watts/cm^2. Not only the current, but also the voltage increases with increasing absorbed power to produce this increased efficiency. The incident power density for our optimum cell is chosen as 1×10^3 watts/cm^2. For a 50 percent efficient converter a heat transfer rate of 5×10^2 watts/cm^2 would be required.

Series Resistance

At high-power densities, the series resistance is one of the most important photovoltaic converter parameters. The vertical junction converter minimizes series resistance by minimizing the current path from the junction to the contact. Figure 10 shows the efficiency as a function of series resistance. As

the series resistance increases from 1 x 10^{-3} ohm to 1 ohm, the efficiency decreases from 53 percent to less than 10 percent. The series resistance chosen for our optimum converter is 1 x 10^{-2} ohms, well above the bulk resistance of 9 x 10^{-5} Ω.

Carrier Concentration

Figure 11 shows the converter efficiency as a function of acceptor concentration for four different donor concentrations. The peak efficiency of 59 percent is reached for both a donor and acceptor concentration of 1 x 10^{17} carriers cm^{-3}. Therefore, for our optimum converter we have chosen both a donor and acceptor concentration of 1 x 10^{17} carriers cm^{-3}.

Surface Recombination Velocity

The effect of surface recombination velocity on the converter efficiency is shown in Figure 12. Increasing the surface recombination velocity on the n-contact surface from 1 cm sec^{-1} to 1 x 10^5 cm sec^{-1} decreases the efficiency from 53 percent to 29 percent. Increasing the surface recombination velocity on the p-contact surface from 1 cm sec^{-1} to 1 x 10^4 cm sec^{-1} decreases the efficiency from 53 percent to 38 percent. Recombination velocities of 5 x 10^2 cm sec^{-1} are required to keep the calculated efficiency above 50 percent. For our optimum converter we have chosen a recombination velocity of 1 x 10^2 cm sec^{-1} (ref. 4) on both the n and p contact surfaces.

CONCLUSIONS

Table II shows the parameter values for our optimum single p-n junction converter. The parameter values chosen for our optimum converter are considered attainable. For example, a converter width of 20 μm was chosen as an attainable dimension, although narrower converters have a higher theoretical efficiency. In reality, a practical device would be composed of multiple p-n junctions connected in series. This has been accomplished previously by mechanically stacking silicon wafers (each containing a p-n junction) and providing a metal contact between each unit (ref. 5); however, the silicon wafers were 240 μm wide. The narrower width of fragile silicon p-n junctions in our proposed converter would probably require a substantially different method of fabrication. It has recently been demonstrated that an epitaxial single crystal composite of silicon and metallic $CoSi_2$ can be fabricated (ref. 6). This opens the possibility of fabricating a series-connected multiple p-n junction device where all the elements of the device, even the metal contacts, are single crystal. The shunt resistance for our optimum converter was realistically chosen as 1 x 10^6 ohm (ref. 4). A converter thickness of 1.5 x 10^{-1} cm will allow for absorption of the 1.06 μm Nd laser radiation. The junction position of 16 μm provides the maximum output for this width converter. Carrier concentrations of 1 x 10^{17} carriers cm^{-3} attain the highest efficiency. The optimized converter has a calculated efficiency of 55 percent for the 1.06 μm Nd laser radiation.

APPENDIX A

MODEL

The model for this vertical junction converter uses the device geometry shown in figure 2 and assumes a generation rate at a depth β given by

$$g(\beta) = \phi_o(1 - Re)\ \alpha e^{-\alpha\beta}$$

where ϕ_o is the number of incident photons [cm^{-2} sec^{-1}]; α is the absorption coefficient [cm^{-1}]; and Re is the reflection coefficient. The basic equations for a n/p device involve the photocurrent from the n and p materials as well as the photocurrent from the depletion region. The currents, when summed, produce the total short circuit current. Following reference 7, we assume that there exists a narrow strip at a depth β below the surface which behaves like a conventional photoconverter. At this depth β, we have the hole excess in the n-region given by

$$D_p \frac{d^2}{dX^2} (P_n - P_{no}) - \frac{(P_n - P_{no})}{\tau_p} = -g(\beta),\ Xj + Xn \leq X \leq B$$

which is subject to the boundary conditions

$$- D_p \frac{d}{dX} (P_n - P_{no}) = S_p(P_n - P_{no})\Big|X = B$$

and

$$P_n - P_{no}\Big|X = Xj + Xn = 0 \quad .$$

This produces the current density

$$Jp = qD_p \frac{d(P_n - P_{no})}{dx}\Bigg|X = X_j + n = -qg(\beta)L_p f(S_p,\ D_p/L_p,\ (B-X_j-X_n)/L_p)$$

where $f(a,b,c) = \frac{a - a \cosh(c) - b \sinh(c)}{b \cosh(c) + a \sinh(c)}$.

Similarly, the electron excess in the p-region is given by

$$D_n \frac{d^2}{dX^2} (n_p - n_{p_o}) - \frac{(n_p - n_{p_o})}{\tau_n} = -g(\beta), \; 0 < X < X_j - X_p$$

with boundary conditions

$$D_n \frac{d}{dX} (n_p - n_{p_o}) = S_n (n_p - n_{p_o}) \Big|_{X = 0}$$

$$n_p - n_{p_o} \Big|_{X = X_j - X_p} = 0 \; .$$

This produces the current density

$$J_n = -qD_n \frac{d}{dX} (n_p - n_{p_o}\Big|_{X = X_j - X_p} = -qg(\beta)L_n f(S_n, D_n/L_n, (X_j - X_p)/L_n)$$

where Xj is the junction depth and Xp, Xn define the space charge region. The photocurrent from the depletion region is neglected, and we have the total short circuit current density as a function of β

$$J_{sc} = J_{sc}(\beta) = J_n(\beta) + J_p(\beta) \; .$$

The total current is obtained by integrating these current densities over the depth of the photoconverter and

$$I_{sc} = \int_0^A J_{sc}(\beta) d\beta \; .$$

Following reference 4, the dark current is given by $I = Ip^* + In^*$ where we have assumed a photoconverter depth in the Z-direction of 1 cm to obtain the dark currents:

$$Ip^* = \frac{gD_p}{L_p} P_{n_o} \; F(\frac{B - X_j - X_n}{L_p}, \frac{S_p L_p}{D_p}) \cdot (e^{qV/kT} - 1)A$$

and

$$I_{n*} = \frac{qD_n}{L_n} n_{p_o} F(\frac{X_j - X_p}{L_n}, \frac{S_n L_n}{D_n}) \cdot [e^{qV/kT}-1]A$$

which gives the injection current

$$I_{inj} = I_{p*} + I_{n*} = I_o (e^{qV/kT}-1) ,$$

where

$$F(A,B) = \frac{B + \tanh(A)}{1 + B \tanh(A)} .$$

Also, from reference 4, we use the recombination current density of

$$J_{rec} = \frac{\pi q n_i W \sinh(\frac{qV}{2kt})}{\sqrt{(\tau_p \tau_n)} q(V_{bi}-V)/kT}$$

where V_{bi} is the built in voltage, n_i is the intrinsic carrier density, W is the width of the depletion region, T is temperature, q is electron charge, τ_p and τ_n are lifetimes, V is voltage, and k is Boltzmann's constant. The short circuit currents and dark currents are used in the equivalent circuit diagrams of figure 3, and we obtain the current voltage relation

$$I(1 + \frac{Rs}{Rsh}) = I_{sc} - V/R_{sh} - I_o[e^{\frac{q(V+IRs)}{kT}} -1] - I_{rec} .$$

which includes the effects of the series resistance R_s and shunt resistance R_{sh}.

Table I

Baseline Parameters

Parameter	Value
Series Resistance	0
Heat Pipe Temperature	20°C
Heat-Transfer Coefficient	100 cal sec^{-} cm^{-} $°C^{-1}$
Surface Recombination Velocity on n-surface	0 cm sec^{-1}
Surface Recombination Velocity on p-surface	0 cm sec^{-1}
Input Power	1×10^{3} w/cm^{2}
Laser Wavelength	1.06 μm
Converter Thickness	1.3×10^{-1} cm
Converter Width	2.0×10^{-3} cm
Converter Length	1 cm
Junction Position	1×10^{-3} cm
Acceptor Carrier Concentration	1.25×10^{17} cm^{-3}
Donor Carrier Concentration	5.0×10^{19} cm^{-3}
Reflection Coefficient	0.05
Shunt Resistance	1×10^{6} ohms

Table II

Parameters for Optimized Converter

Parameter	Value
Series Resistance	1×10^{-2} ohms
Heat Pipe Temperature	20°C
Heat-Transfer Coefficient	40 cal sec^{-1} cm^{-2} $°C^{-1}$
Recombination Velocity on n-Surface	100 cm/sec
Recombination Velocity on p-Surface	100 cm/sec
Input Power	1×10^{3} $watts/cm^{2}$
Laser Wavelength	1.06 μm
Converter Thickness	1.5×10^{-1} cm
Converter Width	20 μm
Converter Length	1 cm
Width of the p-region	16 μm
Acceptor Carrier Concentration	1×10^{17} carriers/cm
Donor Carrier Concentration	1×10^{17} $carriers/cm^{3}$
Reflection Coefficient	0.05
Shunt Resistance	1×10^{6} ohms

REFERENCES

1. DeYoung, R. J.; Tepper, W. D.; Conway, E. J.; and Humes, D. H.: "Preliminary Comparison of Laser and Solar Space Power Systems." Proceedings of the 18th Intersociety Energy Conversion Engineering Conference. Orlando, FLorida; August, 1983; pp. 983-989.

2. Walker, G. H.: "Photovoltaic Conversion of Laser to Electrical Power." Proceedings of the 18th Intersociety Energy Conversion Engineering Conference. Orlando, Florida; August, 1983; pp. 1194-1199.

3. Williams, M. D.; Zapata, L.: "Solar-Pumped Solid State Lasers." NASA TM87615, 1985.

4. Hovel, H. J.: Semiconductors and Semimetals, Volume 11, Solar Cells, Academic Press, 1975.

5. Sater, B. L.; Brandhorst, H. J., Jr.; Riley, T. J.; Hart, R. E., Jr.: "The Multiple Junction Edge-Illuminated Solar Cell," Conference Record of the 10th Photovoltaic Specialist Conference, Nov., 1973, Palo Alto, California, p. 181.

6. Hensel, J. C.; Levi, A. F. J.; Tung, R. T.; and Gibson, J. M.: "Transistor Action in Si/$CoSi_2$/Si Heterostructures," Appl. Phys. Lett. 47, July 15, 1985, p. 151.

7. Grover, A.; Stella, P.: "Vertical Multijunction Solar Cell One Dimensional Analysis," IEEE Transactions on Electron Devices, Vol. ED-21, June, 1974, p. 351-356.

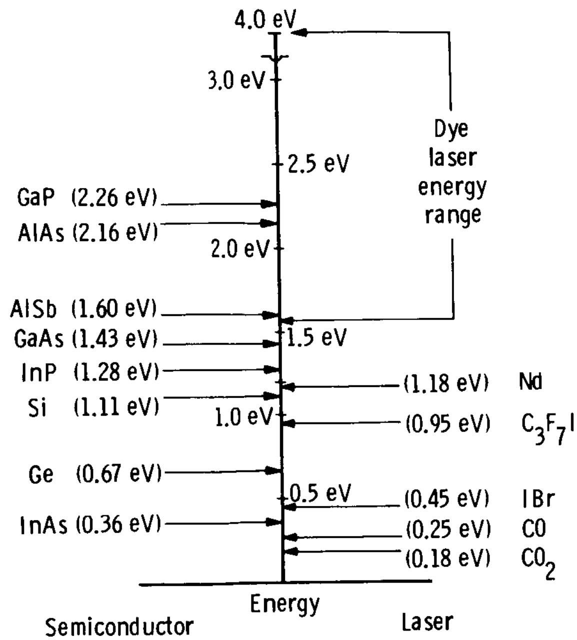

Figure 1 - Semiconductor bandgap energy - laser photon energy relationship

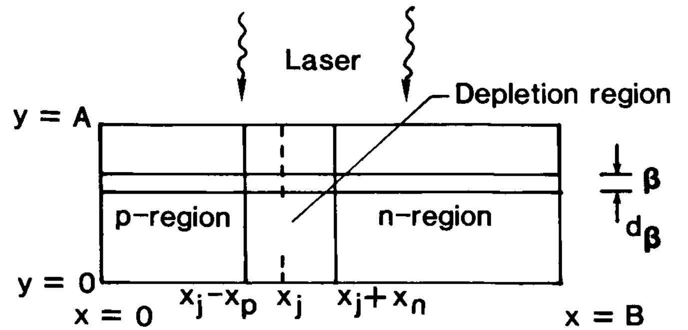

Figure 2 - Converter geometry

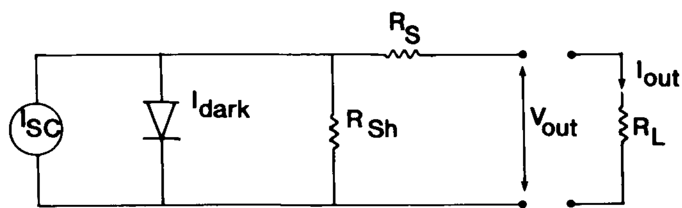

Figure 3 - Equivalent circuit

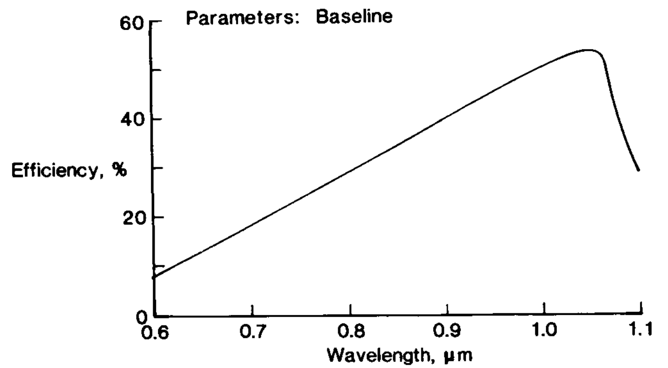

Figure 4 - Converter efficiency vs. laser wavelength

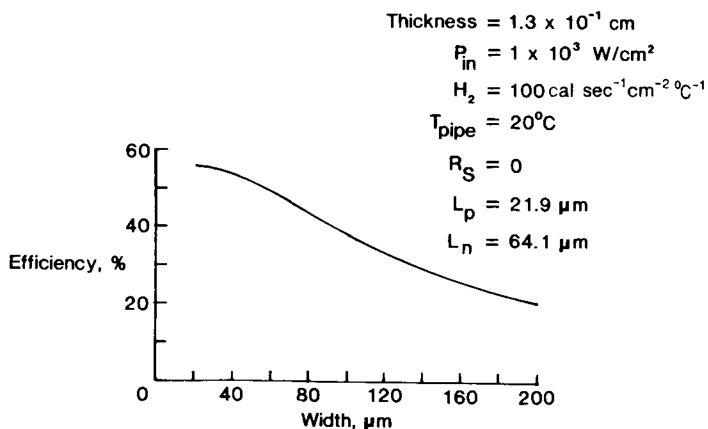

Figure 5 - Converter efficiency vs. converter width

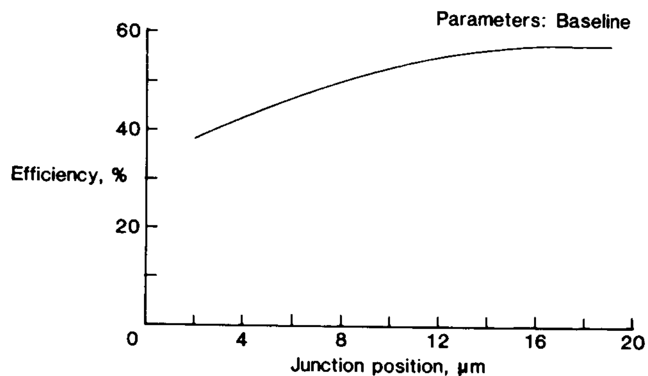

Figure 6 - Converter efficiency vs. junction position for a 20 μm-wide converter

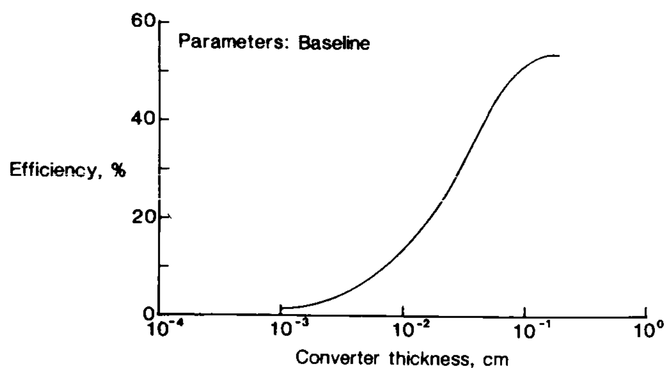

Figure 7 - Converter efficiency vs. thickness

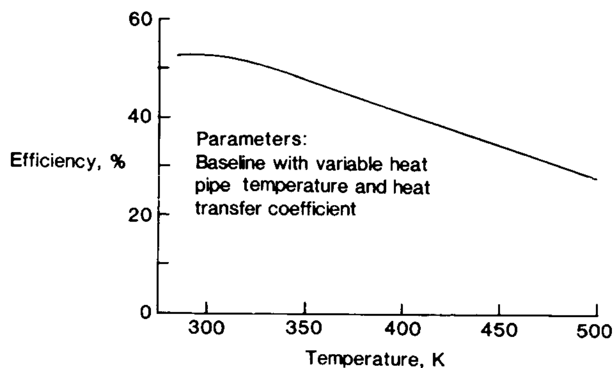

Figure 8 - Converter efficiency vs. temperature

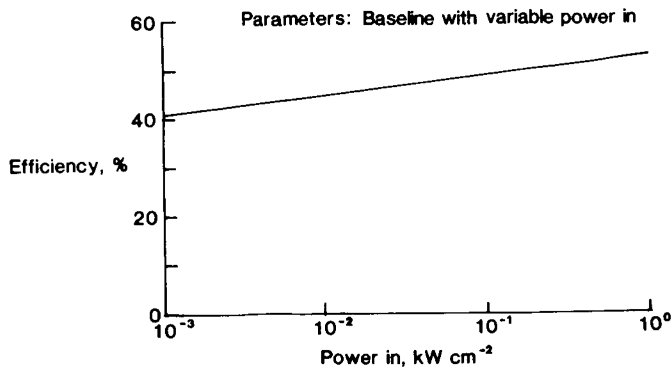

Figure 9 - Converter efficiency vs. input power density

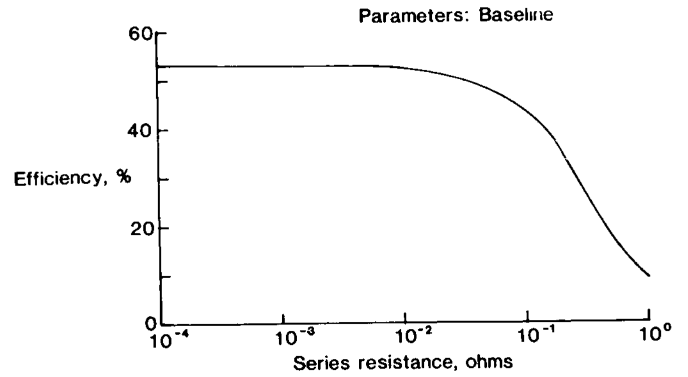

Figure 10 - Converter efficiency vs. series resistance

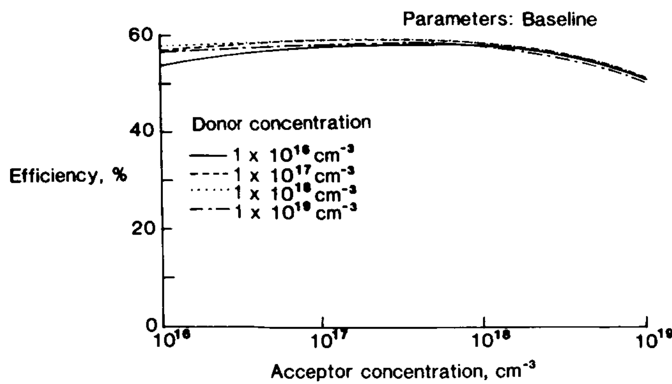

Figure 11 - Converter efficiency as a function of acceptor concentration for four different donor concentrations

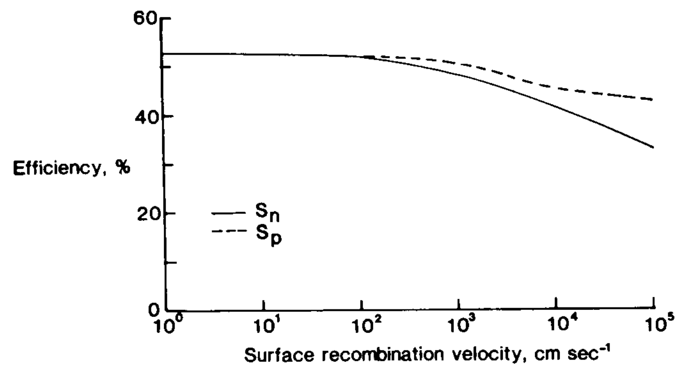

Figure 12 - Converter efficiency vs. surface recombination velocity on the n- and p-contact surfaces